Effect of atomic geometry on shot noise in aluminum quantum point contacts

J. Yao,[1] Y.-C. Chen,[2] M. Di Ventra,[3] and Z. Q. Yang[1],*

[1]*Surface Physics Laboratory (National Key Laboratory), Fudan University, Shanghai 200433, China*
[2]*Department of Electrophysics, National Chiao Tung University, 1001 Ta Hsueh Road, Hsinchu, Taiwan 30010, Republic of China*
[3]*Department of Physics, University of California, San Diego, La Jolla, California 92093-0319, USA*

We investigate the role of atomic geometry on shot-noise properties of aluminum atomic contacts using first-principles calculations. We study both the effect of atomic separation in the wire as well as the geometry of the contacts. We find that shot noise, as opposed to conductance, is very sensitive to atomic details. In particular, the Fano factor for the asymmetric contact structures is more than double that of the symmetric ones due to increased backscattering, and is within the experimental range. These results indicate that shot noise may be used as a tool to infer the atomic geometries of quantum point contacts.

Atomic point contacts can be made using, e.g., mechanically controllable break junctions (MCBJ) or scanning tunneling microscope (STM) techniques.[1] The obtained structures have been extensively studied both experimentally[1–4] and theoretically.[5–12] One issue that has received much less attention is how steady-state current fluctuations (shot noise)[13] are affected by the atomic configurations of nanoscale junctions. This is an important aspect as, in general, the atomic geometry of nanoscale junctions is unknown. In addition, shot noise provides additional information on the transport properties of these systems, such as energy distributions,[14] kinetics of electrons,[15] and correlations of electronic wave functions.[16]

Very few studies have focused on the role of atomic configurations on noise properties. For instance, Lagerqvist *et al.*[17] have performed first-principles calculations of shot-noise properties of parallel carbon wires and found that the Fano factor is quite sensitive to the bonding structure of the wires. Chen and Di Ventra[18] have found that shot noise of Si atomic wires of different lengths oscillates as a function of atoms in the wire.

Shot noise is due to charge quantization[13] and it is, in general, a nonlinear function of the external bias V.[18,19] For mesoscopic systems, shot noise has been related to the transmission coefficients T_n (in the eigenchannel basis, with n the channel index). For a two-terminal geometry in linear response, it can be expressed as[13]

$$S = 4|V|\frac{e^3}{h}\sum_n T_n(1 - T_n),\qquad(1)$$

where e is the electron charge. It is clear from this equation that a fully open (or closed) conducting channel does not contribute to shot noise. It is customary to discuss the Fano factor defined as the ratio of shot noise to its Poisson value $S_p = 2e\langle I\rangle$, where $\langle I\rangle$ is the average dc current,[13]

$$F = S/S_p = \sum_n T_n(1 - T_n)/\sum_n T_n.\qquad(2)$$

An alternative expression for shot noise in terms of single-particle wave functions $\Psi_E^{L,R}(\mathbf{r}, \mathbf{K}_\parallel)$ of left- and right-moving electrons has been derived in Ref. 18 (in atomic units),

$$S = \int_{E_{FL}}^{E_{FR}} dE \left| \int d\mathbf{R} \int d\mathbf{K} \widetilde{I}_{E,E}^{LR} \right|^2,\qquad(3)$$

where $\widetilde{\mathbf{I}}_{E,E}^{LR} = (\Psi_E^L)^* \nabla \Psi_E^R - (\nabla(\Psi_E^L)^* \Psi_E^R$; $d\mathbf{R}$ defines an element of the electrode surface and $\mathbf{K}_\parallel$ is the component of the electron momentum parallel to it. Here we have assumed that a positive bias is applied to the left electrode so that the local Fermi level of the right electrode E_{FR} is higher than that of the left electrode E_{FL}. Expression (3) allows us to calculate shot noise and Fano factor once the single-particle states of the system are known. The equivalence of Eqs. (3) and (1) has been proven in Ref. 17 in the case in which the transmission probabilities T_n are extracted from the single-particle states with independent transverse momenta.

In this paper, we investigate the dependence of shot noise on atomic geometry using aluminum (Al) atomic contacts as a prototypical example. Aluminum has the valence configuration $(3s^23p^1)$ making it thus more interesting than gold in terms of bonding formation and interference between different orbitals. Aluminum atomic contacts have also been studied extensively in experiments.[2–4,20–22] It has been suggested that at least three orbitals contribute to the total conductance, even for the narrowest contacts.[4,21–26] Van den Brom and van Ruitenbeek[27] have measured shot noise of Al contacts and have reported a Fano factor within the range 0.3–0.6.

A schematic of the system investigated is represented in Fig. 1. The first structure we study is a straight three-atom wire connected to four-atom square bases representing an Al(001) surface geometry [see Fig. 1(a)]. The bases are then connected to bulk electrodes which are represented with a semi-infinite jellium model,[24,25,28] with interior electron density close to the value of metallic aluminum ($r_s \approx 2$).[24,25] In this case, we investigate the role of bond stretching on shot noise. We then focus on the geometries of a single atom connected to two Al(001) bases [symmetric structure, Fig. 1(b)] and to one base only [asymmetric structure, Fig. 1(c)], respectively. The results show that when the contact varies from the symmetric structure to the asymmetric one, the
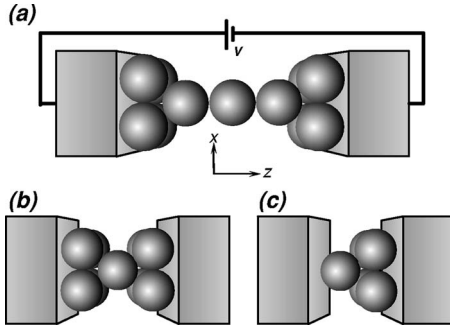
FIG. 1. Schematic of Al quantum point contacts connected to bulk electrodes (gray blocks): (a) a straight three-atom Al wire structure connected to four-atom square bases; (b) a central atom sandwiched between two square bases; (c) a pyramid structure without the left square base.
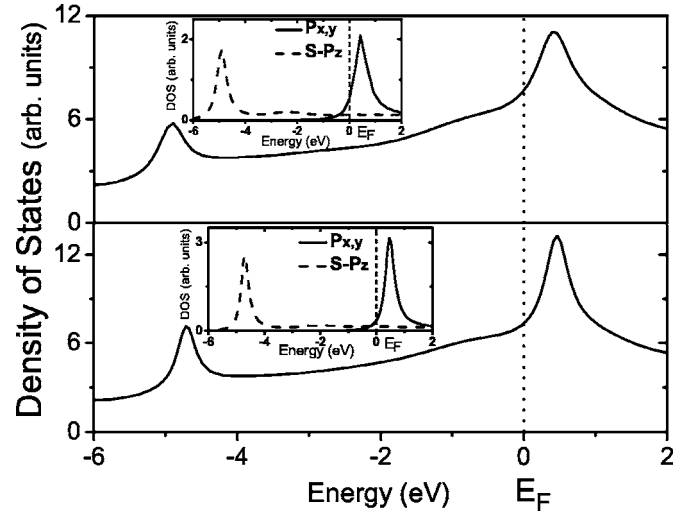

FIG. 2. Top panel: density of states of the unstretched wire of Fig. 1(a). Bottom panel: density of states of the same stretched wire (see text). We denote the left Fermi level as E_F, and set it as zero of energy. The insets are the projected densities of states of the central atoms in the unstretched and stretched wires.

Fano factor more than doubles with a comparatively small reduction in conductance ($\sim 25\%$). The large Fano factor obtained in the asymmetric structure is within the experimentally observed range.[27]

The shot noise is evaluated using Eq. (3) with the stationary scattering wave functions of the whole system calculated by solving the Lippmann-Schwinger equation iteratively to self-consistency. Exchange and correlation are included using the static density-functional theory (DFT) within the local-density approximation (LDA).[17,25,28] More details of the calculations can be found in the original papers in Refs. 17, 25, and 28. Note that since the quantum point contact is made of the same type of metallic atoms, dynamical (viscosity) corrections to the static DFT-LDA conductance are expected to be small, as in the case of gold quantum point contacts.[29] The initial Al-Al atomic bond length and the Al-jellium edge distance are taken as 5.4 a.u. (1 a.u. $\simeq 0.529$ Å) and 2.6 a.u., respectively.[24,25,30] All calculations are done at a bias of 0.01 V, i.e., in the linear regime.

The calculated results for the geometries shown in Fig. 1 are given in Table I. The structure of Fig. 1(a) has a conductance of $1.12G_0$ ($G_0 = 2e^2/h$) and a Fano factor of 0.09. In order to understand these values, we plot in Fig. 2 (top panel) the density of states (DOS) of this structure with the projected density of states (PDOS) of the central atom (inset). The first peak at about -4.9 eV is mainly due to s states while the second at about 0.4 eV comes from the $p_{x,y}$ states, respectively. As the valence configuration of Al is ($3s^2 3p^1$), the wire structure has a σ channel having the characters of s and p_z orbitals,[6] and two degenerate channels with $p_{x,y}$ character.[25] For the $p_{x,y}$ channels, similar to the analysis in

TABLE I. The calculated Fano factors and conductances corresponding to different structures depicted in Figs. 1(a)–1(c). The label "(a)-s" corresponds to the stretched three-atom wire structure of (a).

Structure	(a)	(a)-s	(b)	(c)
Conductance(G_0)	1.12	1.08	4.11	3.16
Fano factor	0.09	0.03	0.13	0.33

Refs. 28 and 31, we note that the contribution to the conductance of a given resonant mode is approximately $G_0 \times \mathrm{DOS}(E_F)/\mathrm{DOS}(E_{peak})$, where $\mathrm{DOS}(E_{peak})$ is the peak value of the line shape of the corresponding resonance, and $\mathrm{DOS}(E_F)$ is the corresponding quantity at the Fermi level. (Since we are treating only the linear-response case, left and right Fermi levels have similar DOS.) Following this argument, the conductance is mainly contributed from the $p_{x,y}$ channels (see the PDOS of the $p_{x,y}$ channels in the inset). The s-p_z channel, on the other hand, has a very small contribution to the transmission. As a result the noise is suppressed.

We now discuss the effect of stretching the wire on conductance and noise. We stretch the atomic wire along the z axis with an increase in Al-Al bond length of $\Delta l = 0.4$ a.u.. The conductance slightly decreases to $1.08G_0$, while the Fano factor is further suppressed to 0.03 (see the column with label "(a)-s" in Table I). The plotted DOS in Fig. 2 (bottom panel) shows a narrower resonant peak above the Fermi levels. This narrowing is due to decreasing interactions between neighboring atoms. From the PDOS of the central atom in the inset, this narrowing thus reduces the ratio $\mathrm{DOS}(E_F)/\mathrm{DOS}(E_{peak})$ in $p_{x,y}$ states, resulting in a reduction of transmissions in the two degenerate channels.

To better understand this trend, we compare the local density of states (LDOS)[32] of the unstretched (top panel) and stretched (bottom panel) wires in Fig. 3. We denote the atoms in the wire as 1, 2, and 3 from left to right. We see that, by stretching the wire, the LDOS of the $p_{x,y}$ orbitals decreases, which is well demonstrated around the central atom. In particular, there is less overlap of the $p_{x,y}$ orbitals between neighboring atoms (see, for instance, the bond structure between atoms 2 and 3). On the other hand, the LDOS of the s-p_z orbitals increases, which is evidently seen from the figures.[33] The decrease (increase) of LDOS for the $p_{x,y}$ (s-p_z) orbitals implies a redistribution of transmissions between these channels. The stretched wire has thus an almost
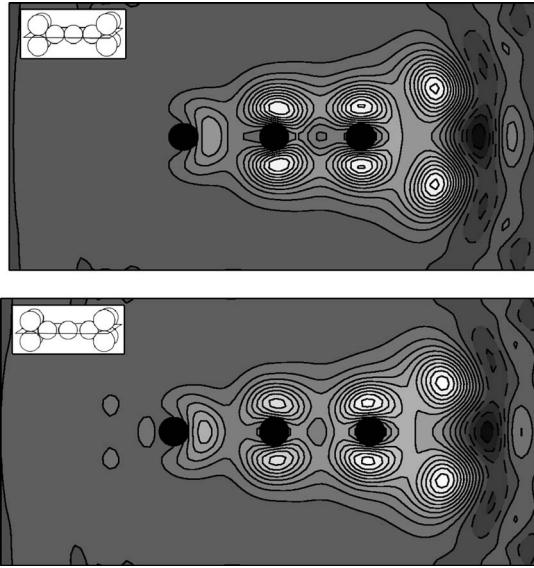
FIG. 3. LDOS of the unstretched (above) and stretched (below) wires (insets show schematic of the wires and the plane where the LDOS is calculated). The black circles indicate the positions of the three atoms. The deep gray regions with dashed lines near the right electrode indicate lower charge density. The contour spacings of the LDOS are the same in both plots.

perfect σ channel and less character from partially open $p_{x,y}$ channels, thus further suppressing the shot noise [see Eq. (1)] compared to the unstretched one.

Let us now move on to the case in which we vary the contact geometry. We illustrate this in Figs. 1(b) and 1(c). The symmetrical structure of the contact [Fig. 1(b)] produces a conductance of $4.11G_0$ with a Fano factor of 0.13 as shown in Table I. Compared with the three-atom wire structure, the conductance and Fano factor both increase. The DOS of this structure is shown as a solid line in Fig. 4. The sharp peaks disappear and broaden to wide and smooth ones due to the strong interactions between the electrodes and the sample atoms. This feature indicates the disappearance of the quasi-one-dimensional character.[34] The Fermi level is now located near the peaks of the $p_{x,y}$ states. Therefore, the conductances
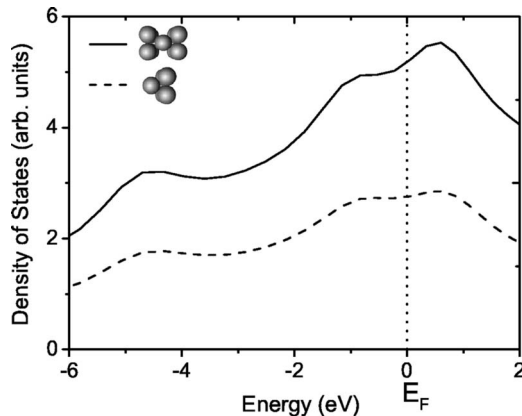

FIG. 4. Density of states of the symmetric (solid line) and asymmetric (dashed line) structures [see Figs. 1(b) and 1(c), respectively].
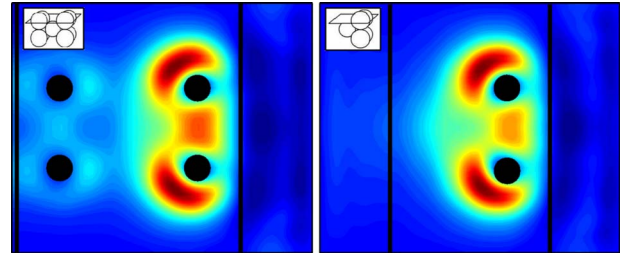

FIG. 5. (Color online) LDOS of the symmetric (left) and asymmetric (right) structures (insets show schematic of the wires and the plane where the LDOS is calculated). The dark vertical lines indicate the surfaces of the jellium electrodes and the black circles denote the positions of the atoms.

contributed from these states are quite substantial, as opposed to the three-atom wire case. On the other hand, while the central atom in the three-atom wire structure makes contact directly along the z axis with neighboring atoms thus providing direct overlap of s, p_z states, there is no such direct overlap in the present case. The s-p_z channel of the central atom thus weakens. The weakening of such a channel is, however, compensated for by the next-neighbor interaction[26] between the two square bases. From the LDOS of the structure in Fig. 5 (left panel), it is clear that the interaction between those base atoms is mostly of π type.

Removing the left square base, we form an asymmetric structure [see Fig. 1(c)]. The conductance of this structure decreases to $3.16G_0$ while the Fano factor is enhanced to 0.33 (Table I). This reduction in conductance is roughly in agreement with the decrease in DOS at the Fermi level[25,28] (see Fig. 4, dashed line). However, the shape of the DOS is quite similar to the one of the symmetric structure, which indicates that the weight of the different types of orbitals does not vary substantially at each energy. The uniformity of the left electrode without base yields less directional spatial LDOS, thus decreasing the interactions between the right square base and the left jellium electrode. This is evident in the LDOS of this structure as plotted in Fig. 5 (right panel). Unlike the π-like interactions between these base atoms in the symmetric structure (Fig. 5, left panel), the right base in the asymmetric structure mainly interacts with the central atom, reducing the hopping between the left electrode and the right base. The breaking of symmetry between the right and left electrodes thus introduces additional backscattering, which reduces the conductance and introduces additional noise with a consequent increase in the Fano factor. The calculated Fano factor for this asymmetric structure is within the range of experimental data as reported in Refs. 20 and 27. We have also calculated the shot noise and conductance for structures with Al (111) surface orientations, and found the same trend. The behavior may indicate that Al atomic contacts fabricated using the MCBJ method[1] may lack ideally symmetric neck structures. This behavior is consistent with the result of final breaking geometries of Al junctions obtained with total energy calculations.[35]

In conclusion, we studied the geometrical effects on shot-noise properties of two common types of Al atomic contacts. Our study revealed that shot noise is more sensitive to atomic arrangements than the conductance itself. The results

therefore indicate that shot noise may provide a tool to infer atomic configurations in atomic-scale junctions.

*Email address: zyang@fudan.edu.cn.

[1] See, e. g., N. Agraït, A. L. Yeyati, and J. M. van Ruitenbeek, Phys. Rep. **377**, 81 (2003), and references therein.

[2] J. I. Mizobata, A. Fujii, S. Kurokawa, and A. Sakai, Phys. Rev. B **68**, 155428 (2003).

[3] A. Halbritter, Sz. Csonka, O. Yu. Kolesnychenko, G. Mihály, O. I. Shklyarevskii, and H. van Kempen, Phys. Rev. B **65**, 045413 (2002).

[4] E. Scheer, N. Agraït, J. C. Cuevas, A. L. Yeyati, B. Ludoph, A. Martín-Rodero, G. R. Bollinger, J. M. van Ruitenbeek, and C. Urbina, Nature (London) **394**, 154 (1998).

[5] G. Taraschi, J. L. Mozos, C. C. Wan, H. Guo, and J. Wang, Phys. Rev. B **58**, 13138 (1998).

[6] J. C. Cuevas, A. L. Yeyati, and A. Martín-Rodero, Phys. Rev. Lett. **80**, 1066 (1998).

[7] Y. Fujimoto and K. Hirose, Phys. Rev. B **67**, 195315 (2003); K. Hirose, N. Kobayashi, and M. Tsukada, *ibid.* **69**, 245412 (2004).

[8] Y.-C. Chen and M. Di Ventra, Phys. Rev. Lett. **95**, 166802 (2005).

[9] M. Di Ventra, Y.-C. Chen, and T. N. Todorov, Phys. Rev. Lett. **92**, 176803 (2004).

[10] N. D. Lang, Phys. Rev. B **55**, 4113 (1997).

[11] Z. Yang, M. Chshiev, M. Zwolak, Y.-C. Chen, and M. Di Ventra, Phys. Rev. B **71**, 041402(R) (2005).

[12] Y.-C. Chen, M. Zwolak, and M. Di Ventra, Nano Lett. **3**, 1691 (2003); **4**, 1709 (2004); **5**, 621 (2005).

[13] For a review, see Ya. M. Blanter and M. Büttiker, Phys. Rep. **336**, 1 (2000).

[14] O. M. Bulashenko, J. M. Rubí, and V. A. Kochelap, Phys. Rev. B **62**, 8184 (2000).

[15] R. Landauer, Nature (London) **392**, 659 (1998).

[16] T. Gramespacher and M. Büttiker, Phys. Rev. Lett. **81**, 2763 (1998).

[17] J. Lagerqvist, Y.-C. Chen, and M. Di Ventra, Nanotechnology **15**, S459 (2004).

[18] Y.-C. Chen and M. Di Ventra, Phys. Rev. B **67**, 153304 (2003).

[19] Y. Wei, B. Wang, J. Wang, and H. Guo, Phys. Rev. B **60**, 16900 (1999).

[20] H. E. van den Brom and J. M. van Ruitenbeek, Phys. Rev. Lett. **82**, 1526 (1999).

[21] J. C. Cuevas, A. Levy Yeyati, A. Martín-Rodero, G. R. Bollinger, C. Untiedt, and N. Agraït, Phys. Rev. Lett. **81**, 2990 (1998).

[22] E. Scheer, P. Joyez, D. Esteve, C. Urbina, and M. H. Devoret, Phys. Rev. Lett. **78**, 3535 (1997).

[23] S. Okano, K. Shiraishi, and A. Oshiyama, Phys. Rev. B **69**, 045401 (2004).

[24] N. Kobayashi, M. Aono, and M. Tsukada, Phys. Rev. B **64**, 121402(R) (2001).

[25] N. D. Lang, Phys. Rev. B **52**, 5335 (1995); N. D. Lang and M. Di Ventra, *ibid.* **68**, 157301 (2003).

[26] J. J. Palacios, A. J. Pérez-Jiménez, E. Louis, E. SanFabián, and J. A. Vergés, Phys. Rev. B **66**, 035322 (2002).

[27] H. E. van den Brom and J. M. van Ruitenbeek, in *Statistical and Dynamical Aspects of Mesoscopic Systems*, edited by D. Reguera, G. Platero, L. L. Bonilla, and J. M. Rubí (Springer-Verlag, Berlin, 2000), p. 114.

[28] M. Di Ventra and N. D. Lang, Phys. Rev. B **65**, 045402 (2001); Z. Yang, A. Tackett, and M. Di Ventra, *ibid.* **66**, 041405(R) (2002).

[29] N. Sai, M. Zwolak, G. Vignale, and M. Di Ventra, Phys. Rev. Lett. **94**, 186810 (2005).

[30] N. D. Lang, Phys. Rev. B **49**, 2067 (1994).

[31] N. D. Lang and Ph. Avouris, Phys. Rev. B **64**, 125323 (2001).

[32] The LDOS is the difference between the local density of states of the complete system and the bare electrodes. It is integrated between the right and left Fermi levels.

[33] Note that the density between atoms 2 and 3 along the z direction in the stretched wire is higher than that in the unstretched one, although there are more contour lines around the middle point between atoms 2 and 3 for the unstretched wire. The contribution from the s-p_z states decreases when approaching the middle point in the unstretched wire, as opposed to the stretched one.

[34] T. Ono and K. Hirose, Phys. Rev. B **70**, 033403 (2004).

[35] P. Jelínek, R. Pérez, J. Ortega, and F. Flores, Phys. Rev. B **68**, 085403 (2003).